Title

High Frequency Radiofrequency Elecromagnetic Fields inside a Conductn Sphere

Authors

Keltner, J.R.
Carlson, J.W.
Roos, M.S.
et al.

Publication Date

1990-07-01

LBL-29413
Preprint

Lawrence Berkeley Laboratory
UNIVERSITY OF CALIFORNIA

Submitted to Magnetic Resonance in Medicine

High Frequency Radiofrequency Electromagnetic Fields inside a Conducting Sphere

J.R. Keltner, J.W. Carlson, M.S. Roos,
S.T.S. Wong, T.L. Wong, and T.F. Budinger

July 1990

Donner Laboratory
Biology & Medicine Division

Prepared for the U.S. Department of Energy under Contract Number DE-AC03-76SF00098.

DISCLAIMER

LBL-29413

High Frequency Radiofrequency Electromagnetic Fields inside a Conducting Sphere

J.R. Keltner, M.S. Roos, S.T.S. Wong,
T.L. Wong, and T.F. Budinger
Research Medicine and Radiation Biophysics Division
Lawrence Berkeley Laboratory
University of California
Berkeley, CA 94720

and

J.W. Carlson
Radiological Imaging Laboratory
University of California
400 Grandview Drive
South San Francisco, CA 94080

This work was supported by the Director, Office of Energy Research,
of the U.S. Department of Energy under Contract No. DE-AC03-76SF00098,
by the National Heart, Lung and Blood Institute under grant HL 25840,
grant HL 07367, and by the International Business Machines Corporation.

Abstract

A high frequency solution of the electromagnetic field produced by a circular surface coil adjacent to a homogeneous conducting, dielectric sphere is used to predict the attainable signal to noise ratio (S/N) and specific absorption rate (SAR) for *in-vivo* ^{1}H NMR spectroscopy experiments from 200 MHz to 430 MHz (4.7 - 10 T). At frequencies above 200 MHz the S/N increases more rapidly with frequency and the SAR increases less rapidly compared with the respective S/N and SAR frequency dependence below 200 MHz. The difference in frequency dependence is due to dielectric resonances of the magnetic field inside the sphere at frequencies above 200 MHz. It is predicted that surface coil NMR experiments may be performed on a head-sized sphere, having conductivity and relative dielectric constant of brain, at frequencies up to 430 MHz without exceeding 8 W/kg local SAR and 3.2 W/kg SAR. The calculations of the S/N and SAR are used to determine optimum surface coil geometries for NMR experiments. Asymmetries in the magnetic field inside the sphere and the power radiated by the surface coils are significant at high frequency. Experimental measurements of the magnetic field inside a head-sized sphere verify the presence of dielectric resonances at frequencies above 200 MHz.

Introduction

The signal to noise ratio and the spectral resolution may be improved by performing experiments at fields much higher than presently available. A particular concern of high field spectroscopy experiments employing surface coil transmitters is power deposition in superficial regions of the patient from the radiofrequency (RF) magnetic fields. Previous work has sought to determine under what conditions are the benefits of high fields outweighed by increased power deposition (1, 2, 3). The present analysis expands upon this work by addressing the feasibility of surface coil NMR experiments at frequencies in the range of 200 to 430MHz (^{1}H at 4.7 - 10 T). The primary goal of this analysis is to estimate the signal to noise ratio (S/N) and absorbed power per unit mass (specific absorbtion rate - SAR) in human head spectroscopy experiments.

As a step toward predicting the performance of surface coils on the human head, the electromagnetic field inside a homogeneous sphere is calculated by solving the inhomogeneous boundary value problem of a loop of uniform current adjacent to a homogeneous conducting sphere. The sphere's parameters are chosen to model human brain: the relative dielectric constant is $\epsilon_r = 2000 f^{-0.75}$ below 140 MHz and $\epsilon_r = 50$ above 140 MHz; in both cases the conductivity is $\sigma = 0.5 f^{0.1}$ S/m (4). A symplifying assumption is that the current on the coil is uniform and independent of the adjacent sphere. The S/N and SAR for NMR experiments are obtained from this solution for the electromagnetic field inside the sphere. This model does not include layers of skin, fat, skull, and cerebrospinal fluid which may have internal fields and SAR much different from the homogeneous sphere.

At frequencies above 200 MHz the S/N increases more rapidly with frequency and the SAR increases less rapidly compared with the respective S/N and SAR frequency dependence below 200 MHz.. The improved frequency dependence is due to dielectric resonances of the magnetic field inside the sphere at frequencies above 200 MHz. Surface coil NMR experiments performed on a head-sized sphere consisting of brain at frequencies up to 430 MHz are predicted to satisfy the Food and Drug Administrations safety guidelines of 8 W/kg for SAR_L and 3.2 W/kg for SAR in human heads (5). Optimum surface coil geometries for NMR experiments are determined using the calculations of the S/N and SAR. Asymmetries in the magnetic field inside the sphere and the power radiated by the surface coils are shown to be significant at high frequency. Experimental measurements of the magnetic field inside a head-sized sphere verify the presence of dielectric resonances at frequencies above 200 MHz.

High Frequency Solution

The high frequency solution for the magnetic field produced by a surface coil adjacent to a homogeneous sphere has been found by solving the inhomogeneous boundary value problem of a ring of radius R carrying uniform current I adjacent to a conducting, dielectric sphere of radius a centered at the origin of a spherical coordinate system (Fig. 1). The centers of the co-axial ring and sphere are separated by distance z. From a multipole expansion of the electromagnetic field (6), the components of the magnetic field B inside the sphere may be expressed as

$$B_r(r,\theta) = \frac{\mu_o I}{4\pi} \sum_{l=1}^{\infty} A_l \sqrt{\frac{l(l+1)(2l+1)}{4\pi}} P_l(cos\theta) \frac{j_l(kr)}{kr} \qquad [1]$$

$$B_\theta(r,\theta) = -\frac{\mu_o I}{4\pi}\sum_{l=1}^{\infty} A_l \sqrt{\frac{2l+1}{4\pi l(l+1)}} sin\theta \frac{dP_l(cos\theta)}{dcos\theta}\left((l+1)\frac{j_l(kr)}{kr} - j_{l+1}(kr)\right) \quad [2]$$

$$B_\phi(r,\theta) = 0, \quad [3]$$

where k is the wave number inside the sphere,

$$k^2 = \epsilon_r \frac{\omega^2}{c^2} + i\mu_o\omega\sigma; \quad [4]$$

A_l is a coefficient determined by the surface coil geometry; ω is the angular frequency; ϵ_r is the relative dielectric constant; c is the speed of light; μ_o is the permeability of free space; $P_l(cos\theta)$ is a Legendre polynomial; and $j_l(kr)$ is a spherical Bessel function of the first kind. The time dependence $e^{-i\omega t}$ is not explicitly written. It is assumed the current distribution on the surface coil is uniform so azimuthal symmetry is preserved and B_ϕ is zero. Only the TE radiation modes need be considered if the source of the field is an oscillating current without free charges.

The current density $\vec{J}$ induced in the sphere is obtained with Ampere's law,

$$J_\phi(r,\theta) = \frac{\mu_o I}{4\pi}\frac{i\omega\sigma}{k}\sum_{l=1}^{\infty} A_l \sqrt{\frac{2l+1}{4\pi l(l+1)}} j_l(kr) sin\theta \frac{dP_l(cos\theta)}{dcos\theta}, \quad [5]$$

where σ is the conductivity. The power deposited in the sphere P is obtained from integrating $\vec{J}^2/2\sigma$ over the volume of the sphere,

$$P = \frac{\mu_o I^2 \omega a^2}{32\pi^2 \mid k \mid^2}\sum_{l=1}^{\infty} \mid A_l \mid^2 Im[kj_l^*(ka)j_{l+1}(ka)], \quad [6]$$

where Im gives the magnitude of the imaginary part of the complex quantity inside the brackets.

The A_l are found by satisfying the boundary conditions of the magnetic field at the surface of a homogeneous conducting, dielectric sphere given an incident magnetic field produced by an

adjacent ring of uniform current (6):

$$A_l = 2\pi\sqrt{\frac{4\pi(2l+1)}{l(l+1)}}\frac{K^2R^2h_l^{(1)}(K\sqrt{z^2+R^2})}{\sqrt{z^2+R^2}}\frac{dP_l(\xi)}{d\xi} \times\frac{k\left(j_l(Ka)y_{l+1}(Ka)-y_l(Ka)j_{l+1}(Ka)\right)}{kh_l(Ka)j_{l+1}(ka)-Kj_l(ka)h_{l+1}(Ka)}, \quad [7]$$

where K is the wave number in free space; y_l are spherical Bessel functions of the second kind; h_l are spherical Bessel functions of the third kind; and ξ is the cosine of the angle subtended by the loop: $\xi = z/\sqrt{z^2+R^2}$.

Previous work by one of the authors used a combined quasi-static/multipole solution for B_r to analyze S/N and SAR below 200 MHz (1). The previous combined quasi-static/multipole solution and the completely multipole high frequency solution presented here differ by up to 10% in S/N and 20% in SAR at 430 MHz. The quasi-static/multipole solution is given by [1] to [6] with

$$A_l^q = 2\pi\sqrt{\frac{4\pi(2l+1)}{l(l+1)}}\frac{R^2}{(z^2+R^2)^{(\frac{l}{2}+1)}}\frac{dP_l(\xi)}{d\xi}\times\frac{a^{l-1}}{j_{l-1}(ka)}. \quad [8]$$

The time averaged power radiated P_{rad} by a loop adjacent to an object in free space is calculated by integrating the Poynting vector over an arbitrary surface surrounding the loop and the object (6). The time averaged radiated power is

$$P_{rad} = \frac{c\mu_o I^2}{32\pi^2 \mid K \mid^2}\sum_l \mid D_l \mid^2, \quad [9]$$

where

$$D_l = 2\pi\sqrt{\frac{4\pi(2l+1)}{l(l+1)}}\frac{K^2R^2h_l^{(1)}(K\sqrt{z^2+R^2})}{\sqrt{z^2+R^2}}\frac{dP_l(\xi)}{d\xi} \times\left(\frac{j_l(K\sqrt{z^2+R^2})}{h_l(K\sqrt{z^2+R^2})}-\frac{kj_l(Ka)j_{l+1}(ka)-Kj_l(ka)j_{l+1}(Ka)}{kh_l(Ka)j_{l+1}(ka)-Kj_l(ka)h_{l+1}(Ka)}\right). \quad [10]$$

The signal to noise ratio in a plane perpendicular to the static magnetic field for $T_r >> T_1$ and constant bandwidth (7) is

$$\text{S/N} \propto \frac{\omega^2 \mid B_r - iB_\theta \mid}{\sqrt{P + P_{rad}}}. \qquad [11]$$

The power radiated by the coil is included in the calculation of S/N to approximate additional coupling of the surface coil to the patient via radiation reflected by the RF shield inside the magnet. The local SAR is

$$\text{SAR}_L = \frac{\mid \vec{J} \mid^2}{2\sigma\rho}, \qquad [12]$$

where ρ is the density of the sphere. The total SAR is the power deposited in the sphere divided by the mass of the sphere:

$$\text{SAR} = \frac{P}{\rho V}, \qquad [13]$$

where V is the volume of the sphere.

Results

FREQUENCY DEPENDENCE OF S/N AND SAR:

For a voxel on the axis of the coil 5 cm deep into a 20 cm diameter sphere, the S/N dependance upon frequency for a 12 cm diameter coil displaced 2 cm from the sphere improves from an approximately linear relationship below 200 MHz to a 1.4 power law relationship between 200 and 430 MHz (Fig. 2). For voxels closer to the surface of the sphere, the high frequency dependence is more linear. For voxels closer to the center of the sphere, the high frequency dependence is a slightly higher power law.

In the coil and sphere geometry used above and a 5 cm deep voxel, SAR_L and SAR increase quadratically with frequency below 100 MHz, linearly up to 300 MHz, and with negative curvature above 300 MHz (Fig. 3). For voxels closer to the surface of the sphere, the frequency dependence remains linear from 100 MHz to 430 MHz. For voxels closer to the center of the sphere, the frequency dependence has larger negative curvature above 300 MHz.

PREDICTED SAR:

The SAR_L and SAR calculated in this high frequency solution may be used to estimate the maximum SAR_L and the SAR for surface coil NMR experiments on human heads. In the following estimates a 75 μs RF magnetic field pulse with T_r = 0.4 s rotates the ^1H dipole moments in the voxel being examined by the Ernst angle of 35°. The T_1 of the ^1H is assumed to be 2 seconds and the maximum flip angle deviation over the ^1H chemical shift at 10 T is 4.1%. The radii of the surface coils used in the estimates are the optimum radii for the given frequency and the depth of the voxel being examined. The maximum SAR_L for a voxel 1 cm deep increases with frequency from 0.02 W/kg at 64 MHz to 0.5 W/kg at 430 MHz. The maximum SAR_L for a voxel 5 cm deep increases with frequency from 0.08 W/kg at 64 MHz to 1.3 W/kg at 430 MHz. For a voxel 1 cm deep the SAR increases to 0.02 W/kg at 430 MHz, and for a voxel 5 cm deep the SAR increases to 0.07 W/kg at 430 MHz. For a large loop concentric with the sphere the magnetic field approximates a uniform field; for this loop geometry the high frequency solution predicts SAR's which agree with the head coil data of Röschmann (2).

OPTIMUM COIL DESIGN:

Evaluating the S/N at various coil displacements z (where $z > R$) reveals that the largest S/N

is achieved by placing the plane of the surface coil tangent to the surface of the sphere. The radius of the surface coil which produces the largest S/N increases with voxel depth and frequency. For a voxel depth of 1cm in a 20 cm diameter sphere, the optimum surface coil radius is less than 1 cm up to 430MHz. For a voxel depth of 5 cm, the optimum surface coil radius is R_{opt} = 3.5 cm below 64MHz increasing to R_{opt} = 6 cm at 430 MHz (Fig. 4). For a voxel at the center of the sphere, the optimum surface coil geometry is a coil with large radius. In the limit of low frequency and large sphere radius the high frequency solution presented here reduces to the static field solution for the optimum surface coil radius of a coil adjacent to a infinite half space (8).

The maximum SAR_L falls off rapidly as the radius and displacement of the surface coil increase; thus, a small increase in radius of the surface coil beyond the optimum will only slightly degrade S/N but can greatly reduce the SAR_L. For example at 64 MHz, 170 MHz, and 430 MHz increasing the coil radius 2 cm beyond the optimum radii for a 5 cm depth (3.5 cm, 4 cm, and 6 cm) decreases the S/N by 5%, but decreases SAR_L by 60%, 60%, and 40% respectively.

B1 FIELD DISTRIBUTION:

In an NMR experiment the nuclei do not interact with the complete surface coil magnetic field, but with one of the circularly polarized components of the magnetic field. At high frequencies the magnitude of the circularly polarized components become increasingly asymmetric with respect to the axis of the surface coil (9), leading to an asymmetric NMR signal over the volume of the sphere. At 64 MHz, 170 MHz, and 430 MHz the asymmetry produces up to 15%, 33%, and 70% maximum variation in the NMR signal between two voxels on opposite sides of the surface coil axis, where the percentage variation is (max. field - min. field)/max. field. (Fig. 5).

RADIATED POWER:

Above 200 MHz the power radiated by a coil adjacent to a sphere in free space is a significant percentage of the power deposited in the sphere, increasing to 15% at 400 MHz for a 12 cm diameter coil displaced 2 cm from the sphere (Fig. 6). Details of the power radiated depend upon the environment of the coil. In an NMR experiment most radiated power will be reflected by the conducting surfaces of the magnet and absorbed by the patient.

Experimental Verification of High Frequency Solution

Experimental measurements of the on-axis magnetic field in a 16 cm diameter spherical Pyrex flask containing alternatively deionized water ($\epsilon_r = 80$, $\sigma = 0.0$ S/m) and 0.5% saline ($\epsilon_r = 78$ and $\sigma = 0.82$ S/m) were performed using a 2 cm search coil and a Hewlett Packard 4195A Network/Spectrum Analyzer at 90 MHz, 180 MHz, 370 MHz and 415 MHz. The fields were produced by distributed capacitance surface coils with 9 cm inner diameter, displaced 1 cm from the sphere. The distributed capacitors consisted of pieces of 2.5 cm wide copper foil separated by 2 mm of mylar. The 90 MHz coil contained one distributed capacitor; the 180 MHz coil contained two distributed capacitors; and the 370 - 415 MHz coil contained four distributed capacitors.

The experiments verify the presence of a dielectric resonance in deionized water and an increase in the magnetic field in the hemisphere of the sphere near the coil in 0.5% saline above 200 MHz (Fig. 7). The difference between the predicted and observed results at 415 MHz may

result from non-uniformity of the current distribution on the coils above 200 MHz. A more uniform current distribution could be achieved by driving the coils at more than one point (10). The measurements taken at 370 MHz and 415 MHz were particularly sensitive to loading by the experimentalist and coupling to surface currents on the co-axial cables leading to the spectrum analyzer. Ferrite rings were used to minimize the surface currents on the co-axial cables.

Discussion and Conclusion

Above 200 MHz, the magnetic field inside the sphere exhibits frequency dependent maxima and minima not present in the static solution (Fig. 7). This is similar to the phenomenon of dielectric resonances described in the theory of wave guides and resonant cavities (11). As can be seen from the 0.5% saline plot in Figure 7, at higher frequency the magnetic field in the hemisphere near the coil is larger than the field at lower frequencies. Thus a 12 cm diameter coil producing a 1.00 mT 64 MHz RF magnetic field at its center and a second 12 cm diameter coil producing a 0.77 mT 430 MHz RF magnetic field at its center will both produce a 0.30 mT RF magnetic field 5 cm deep into the sphere, where both coils are displaced 2 cm from the sphere. If a constant flip angle for a voxel at a given depth is desired, the smaller amplitude of the RF magnetic field at high frequency yields the greater than linear dependence of the S/N and less than quadratic dependence of the SAR (Fig. 2 and Fig. 3).

To more accurately predict the maximum SAR_L in a human head requires the incorporation of layers to the sphere model (3). Since cerebrospinal fluid (CSF) is believed to be up to five times

as conducting as brain, the maximum SAR_L in a model including a CSF layer may increase by a large factor. If the CSF layer is thin, then modifications to the magnetic field inside the sphere will be small and the SAR_L will have a linear dependence upon conductivity. With this assumption and the results presented here, one may predict that in a *in-vivo* surface coil NMR experiment using a 12 cm diameter surface coil displaced 2 cm from an approximately 20 cm diameter sphere of brain with a thin outer layer of CSF, a 430 MHz pulse of duration 75 μs, flip angle of 35°, and $T_r = 0.4$ s for a voxel 5 cm deep into the sphere will produce a 6.5 W/kg SAR_L and a 0.35 W/kg SAR. Both of these predictions are within the Food and Drug Administration safety guidelines of 8 W/kg for SAR_L and 3.2 W/kg for SAR in human heads (5).

Acknowledgement

This work was supported by the Director, Office of Energy Research, of the U.S. Department of Energy under Contract No. DE-AC03-76SF00098, by the National Heart, Lung and Blood Institute under grant HL 25840, grant HL 07367, and by the International Business Machines Corporation.

References

1. J.W. Carlson, *J. Mag. Res.* **78**, 563(1988).

2. P. Röschmann, *Med. Phys.* **14**, 922(1987).

3. R.W. Brown, *et al*, *J. Mag. Res.* **80**, 225(1988).

4. R. Pethig and D.B. Kell, *Phys. Med. Biol.* **8**, 933(1987).

5. *Federal Register* **53**, 48981(Dec. 5, 1988).

6. J.D. Jackson, 'Classical Electrodynamics', 2nd ed., John Wiley and Sons, Inc., New York, Ch. 16 (1975).

7. D.I. Hoult and P.C. Lauterbur, *J. Mag. Res.* **34**, 425(1979).

8. C-N Chen and D.I. Hoult, 'Biomedical Magnetic Resonance Technology', Adam Hilger, New York, 161 (1989).

9. G.H. Glover, *et. al.*, *J. Mag. Res.* **64**, 255(1985).

10. S.A. Schelkunoff and H.T. Friis, 'Antennas', John Wiley and Sons, Inc., New York, 503(1952).

11. R.E. Collin, 'Field Theory of Guided Waves', McGraw-Hill, New York (1966).

Figure Captions

Figure 1 Schematic arrangement of a homogeneous conductive sphere near a circular current loop. The sphere is centered at the origin of the spherical coordinate system.

Figure 2 The signal to noise ratio, normalized to its value at 430 MHz, is plotted vs. frequency for a voxel 5 cm into the sphere, on axis. The surface coil has a 12 cm diameter and is displaced 2 cm from the sphere.

Figure 3 The maximum SAR_L and SAR are plotted vs. frequency assuming the coil parameters of Figure 2 for a voxel on axis, 5 cm into the sphere, receiving a 75 μs 35° pulse with T_r = 0.4s.

Figure 4 The signal to noise ratio is plotted vs. the coil displacement and the coil radius for a voxel 5 cm into the sphere, on axis. The signal to noise is normalized to the optimum coil geometry.

Figure 5 Contour plot of one of the circularly polarized B field components inside the sphere produced by a 12 cm diameter coil displaced 2 cm from the sphere. Each isocline represents a 5% drop in the amplitude of the field relative to the amplitude of the field at the edge of the sphere.

Figure 6 The percentage of power radiated compared to power deposited in the sample is plotted vs. frequency for a 12 cm coil displaced 2 cm from the sphere.

Figure 7 Plots of the B field on axis, normalized to the edge of the sphere. Solid lines are theory. Solid dots are observations at 415 MHz and crosses are observations at 180 MHz.

Variables

a	=	lower case A
A	=	upper case A
B	=	upper case B
c	=	lower case C
D_l	=	upper case D sub lower case L
f	=	lower case F
h_l	=	lower case H sub lower case L
I	=	upper case I
j_l	=	lower case J sub lower case L
J	=	upper case J
k	=	lower case K
K	=	upper case K
l	=	lower case L
P_l	=	upper case P sub lower case L
P	=	upper case P
P_{RAD}	=	upper case P sub upper case RAD
r	=	lower case R
R	=	upper case R
R_{opt}	=	upper case R sub lower case OPT
V	=	upper case V
y_l	=	lower case Y sub lower case L
z	=	lower case Z

ϵ_r = lower case greek symbol epsilon sub lower case R

μ = lower case greek symbol mu

μ_o = lower case greek symbol mu sub lower case O

ω = lower case greek symbol omega

ϕ = lower case greek symbol phi

ρ = lower case greek symbol rho

σ = lower case greek symbol sigma

θ = lower case greek symbol theta

ξ = lower case greek symbol xi

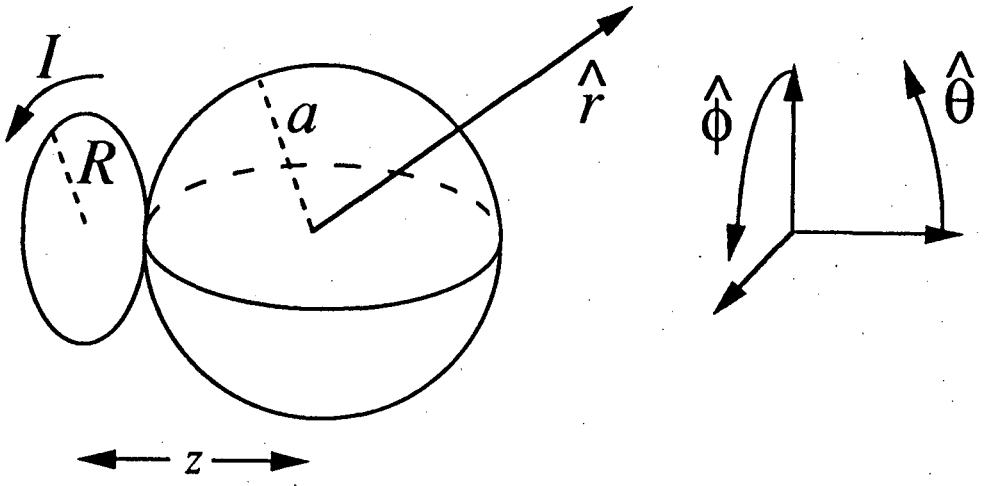

Figure 1

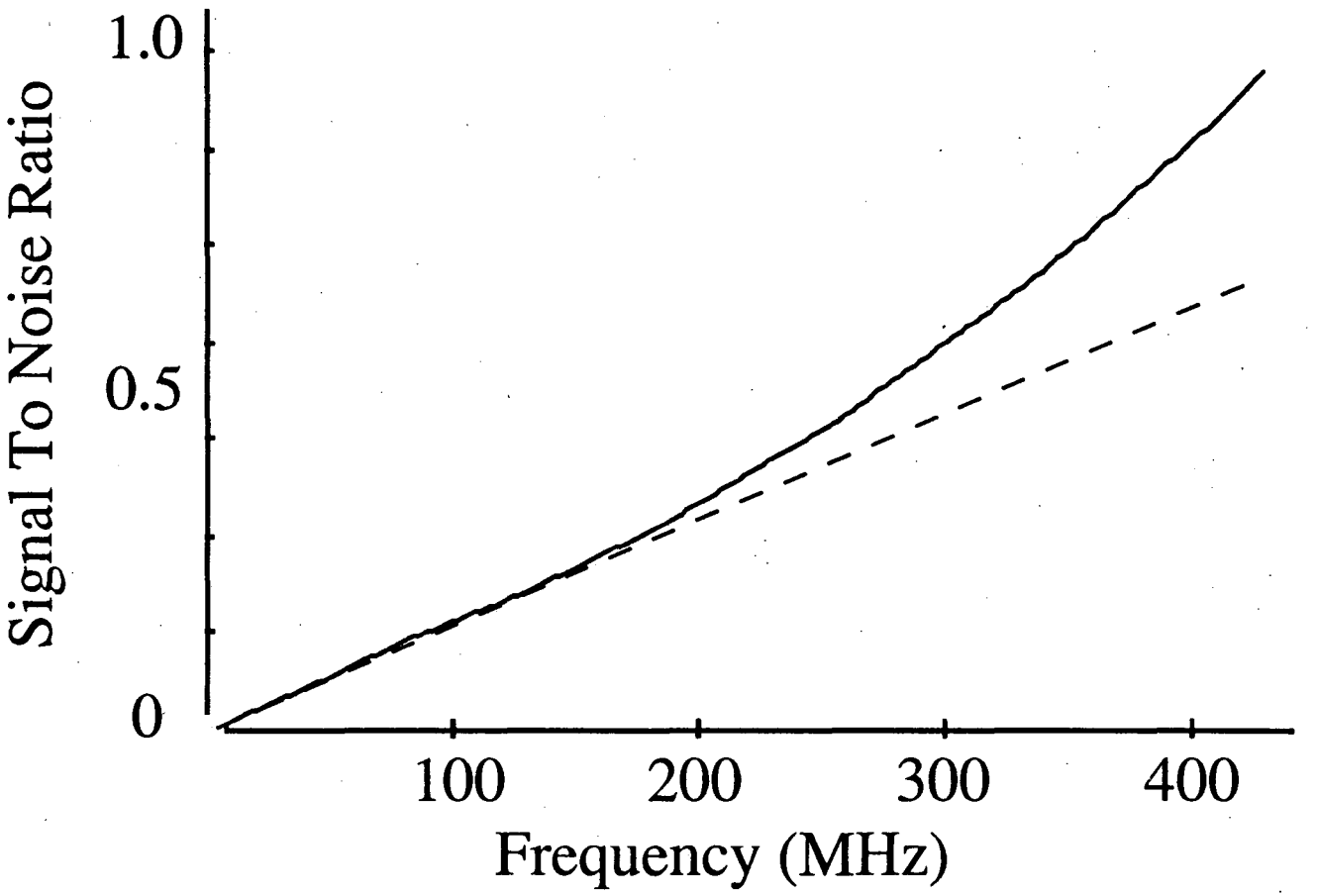

Figure 2

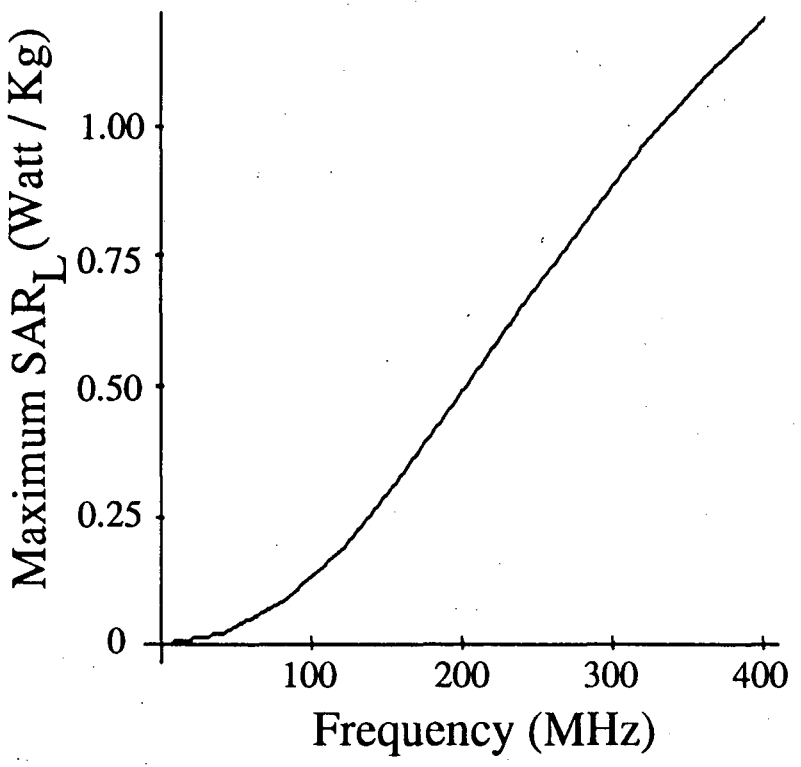
Maximum SAR_L (Watt / Kg)
1.00
0.75
0.50
0.25
0
100
200
300
400
Frequency (MHz)

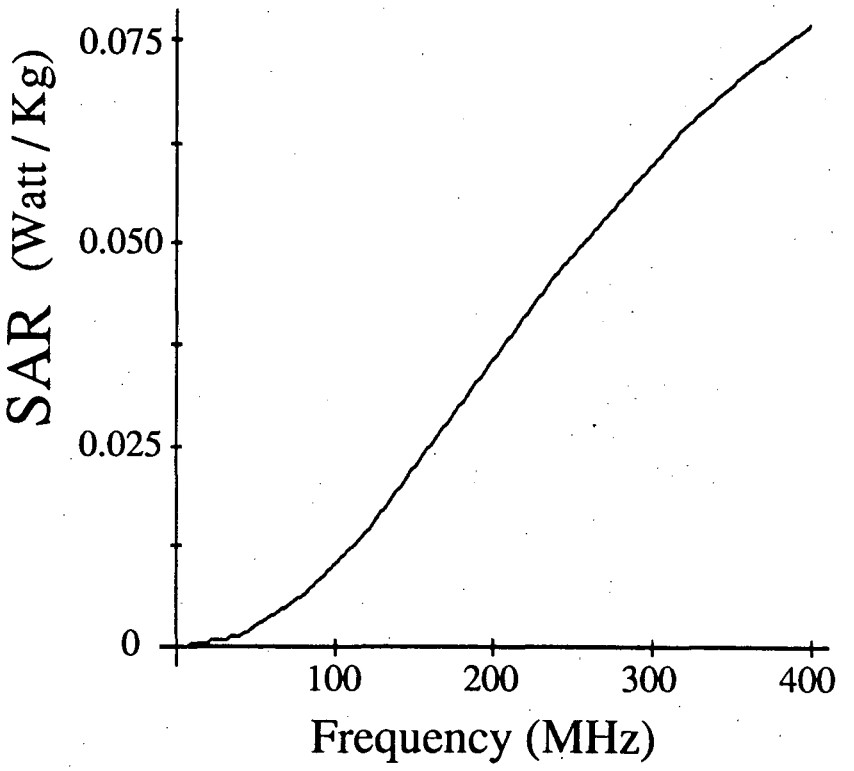
SAR (Watt / Kg)
0.075
0.050
0.025
0
100
200
300
400
Frequency (MHz)

Figure 3

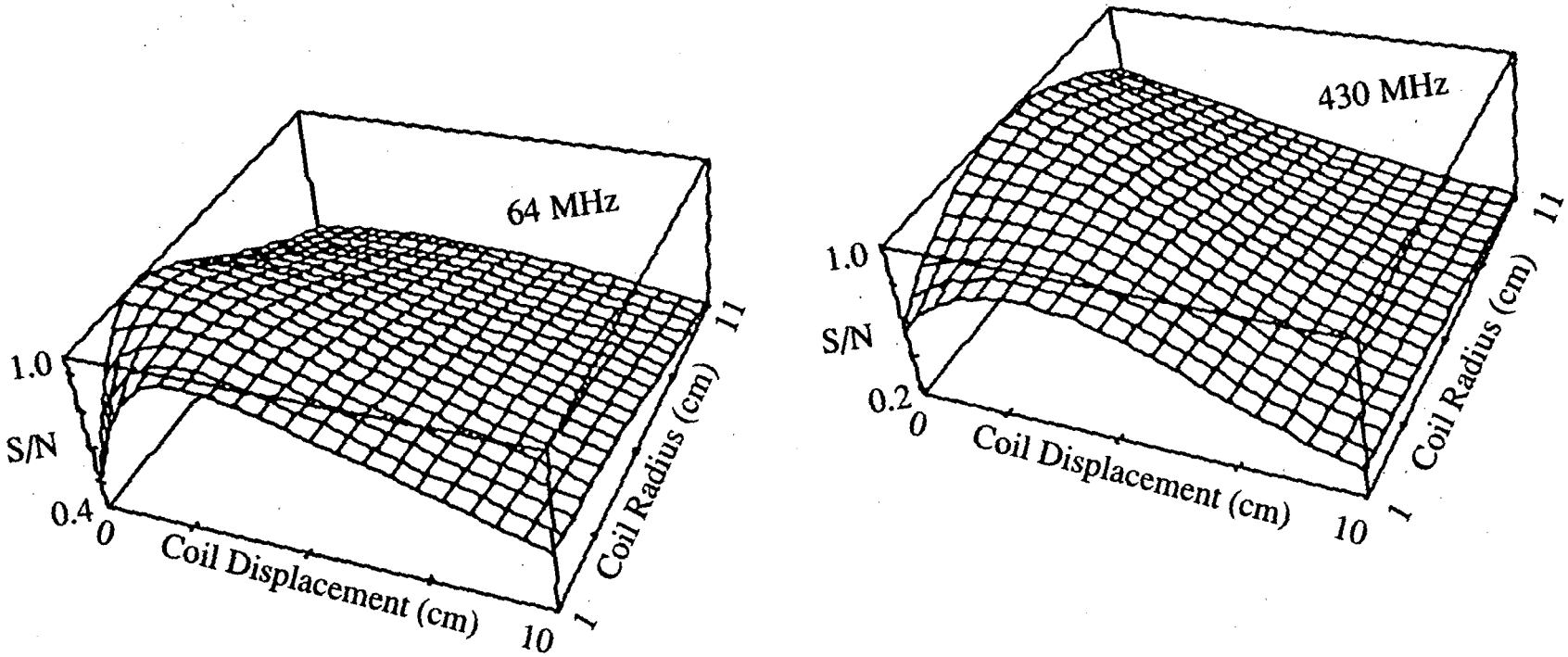
64 MHz
1.0
S/N
0.4
0
Coil Displacement (cm)
10
1
Coil Radius (cm)
11
430 MHz
1.0
S/N
0.2
0
Coil Displacement (cm)
10
1
Coil Radius (cm)
11

Figure 4

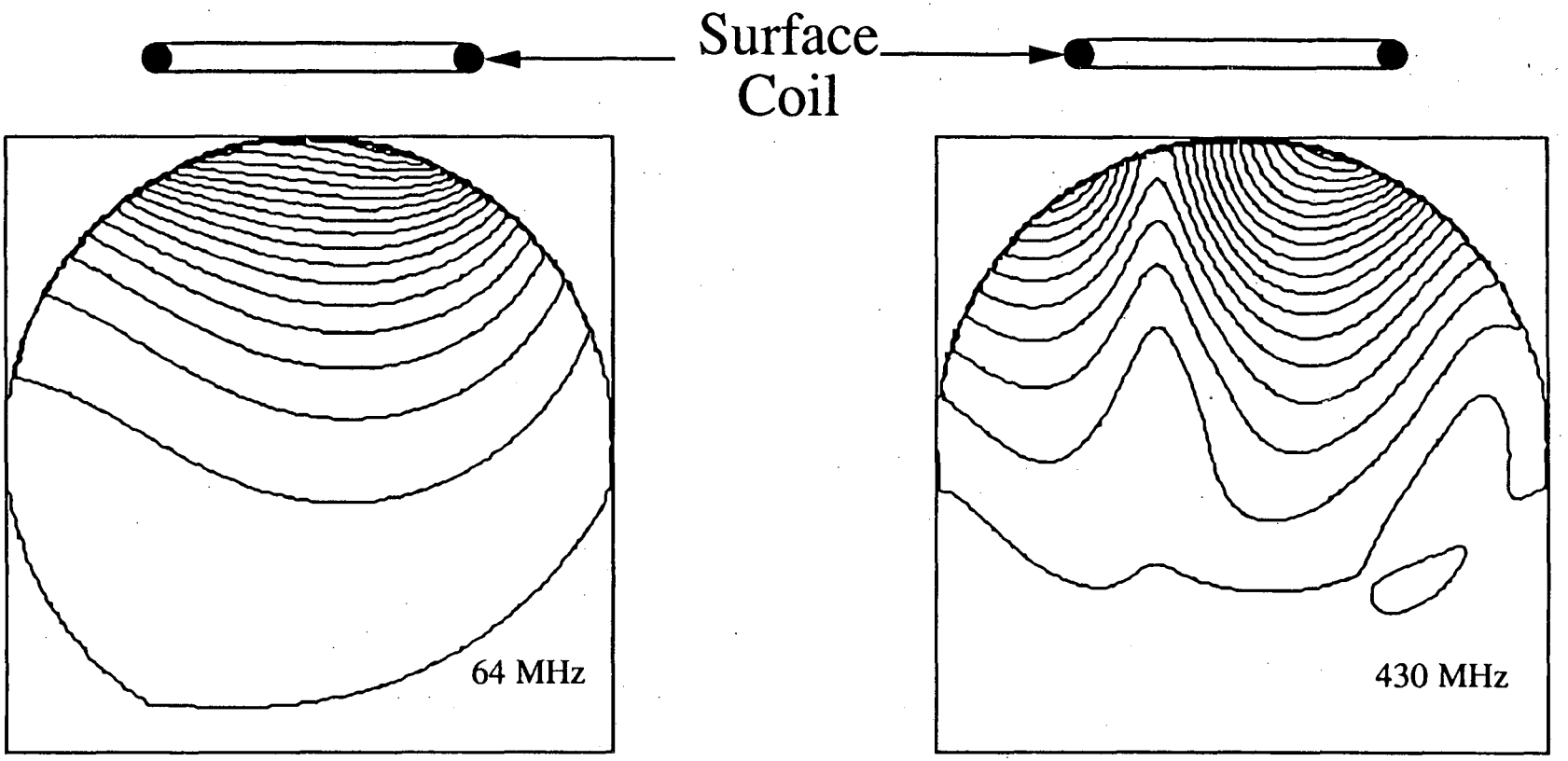

Figure 5

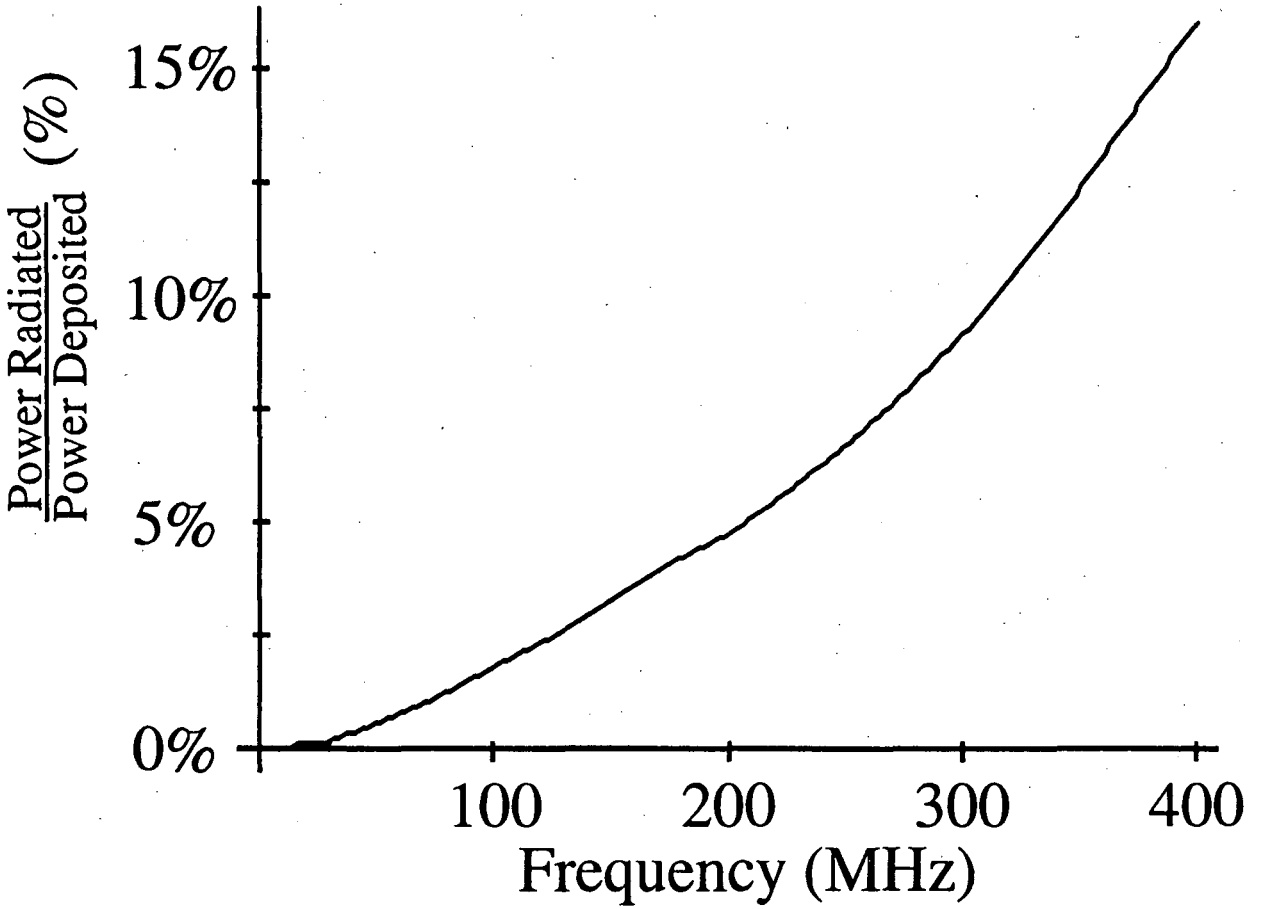
15%
10%
5%
0%
Power Radiated / Power Deposited (%)
100
200
300
400
Frequency (MHz)

Figure 6

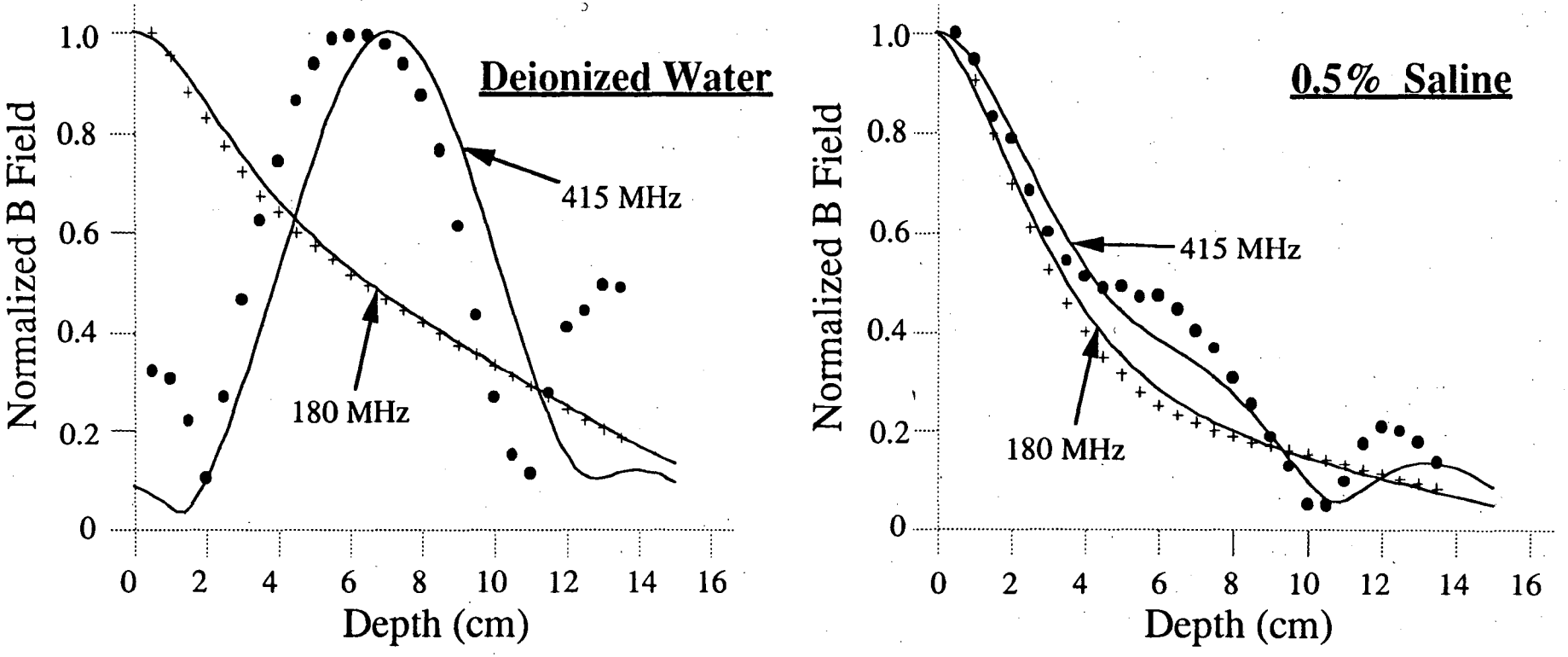
Deionized Water
0.5% Saline
Normalized B Field
Depth (cm)
415 MHz
180 MHz
1.0
0.8
0.6
0.4
0.2
0
0
2
4
6
8
10
12
14
16

Figure 7

LAWRENCE BERKELEY LABORATORY
UNIVERSITY OF CALIFORNIA
INFORMATION RESOURCES DEPARTMENT
BERKELEY, CALIFORNIA 94720